THE JOURNAL OF BIOLOGICAL CHEMISTRY VOL. 286, NO. 45, pp. 39179–39187, November 11, 2011

A Novel NADH-dependent and FAD-containing Hydroxylase Is Crucial for Nicotine Degradation by *Pseudomonas putida*[*] [S]

Received for publication, July 19, 2011, and in revised form, September 23, 2011 Published, JBC Papers in Press, September 23, 2011, DOI 10.1074/jbc.M111.283929

Hongzhi Tang[‡], Yuxiang Yao[‡1], Dake Zhang[§1], Xiangzhou Meng[‡1], Lijuan Wang[‡1], Hao Yu[‡1], Lanying Ma[‡], and Ping Xu[‡2]

From the [‡]State Key Laboratory of Microbial Metabolism & School of Life Sciences and Biotechnology, Shanghai Jiao Tong University, Shanghai 200240, China and [§]Beijing Institute of Genomics, Chinese Academy of Sciences, Beijing 100029, China

Background: The biochemical mechanism of nicotine biodegradation is important.
Results: An NADH-dependent and FAD-containing hydroxylase (HspB) for nicotine degradation was purified and mechanistically characterized.
Conclusion: The hydroxylase is crucial for nicotine degradation by *Pseudomonas putida.*
Significance: The novel HspB provides a sound basis for future studies aimed at a better understanding of the molecular principles of nicotine degradation.

Nicotine, the main alkaloid produced by *Nicotiana tabacum* and other *Solanaceae*, is very toxic and may be a leading toxicant causing preventable disease and death, with the rise in global tobacco consumption. Several different microbial pathways of nicotine metabolism have been reported: *Arthrobacter* uses the pyridine pathway, and *Pseudomonas*, like mammals, uses the pyrrolidine pathway. We identified and characterized a novel 6-hydroxy-3-succinoyl-pyridine (HSP) hydroxylase (HspB) using enzyme purification, peptide sequencing, and sequencing of the *Pseudomonas putida* S16 genome. The HSP hydroxylase has no known orthologs and converts HSP to 2,5-dihydroxypyridine and succinic semialdehyde, using NADH. $^{18}O_2$ labeling experiments provided direct evidence for the incorporation of oxygen from O_2 into 2,5-dihydroxy-pyridine. The *hspB* gene deletion showed that this enzyme is essential for nicotine degradation, and site-directed mutagenesis identified an FAD-binding domain. This study demonstrates the importance of the newly discovered enzyme HspB, which is crucial for nicotine degradation by the *Pseudomonas* strain.

The tobacco manufacturing process produces large quantities of dangerously toxic liquid, solid, and airborne wastes, which cause serious problems because nicotine is extremely toxic (1). In general, the removal of these pollutants from the environment via physicochemical and natural biological processes is relatively slow, unpredictable, or irreversibly toxic to the biosphere. Therefore, the main, if not the only, successful strategy to fight pollution is the use and manipulation of the detoxification abilities of living organisms (2, 3). Soil microorganisms, particularly bacteria of the genus *Pseudomonas*, can metabolize a broad range of toxic compounds, including nicotine (3–5). Thus far, two pathways have been postulated for nicotine degradation by bacteria. The pyridine pathway used by *Arthrobacter oxidans* starts with the hydroxylation of the pyridine ring, and the pyrrolidine ring is opened later (Fig. 1*A*). The genes and enzymes used by *Arthrobacter* are known (4).

The pyrrolidine pathway used by *Pseudomonas* spp. begins with the formation of a double bond in the pyrrolidine ring to give *N*-methylmyosmine. The double bond is hydrolyzed to produce pseudooxynicotine that is oxidized to give 3-succinoylpyridine and methylamine. The 3-succinoylpyridine is then hydroxylated to yield 6-hydroxy-3-succinoylpyridine (HSP),[3] which is converted to 2,5-dihydroxy-pyridine (DHP) and succinate (6, 7) (Fig. 1*B*). HSP and DHP are useful precursors for chemical synthesis (8). In the human body, there are at least six different pathways for the metabolism of nicotine, one of which is similar to the pyrrolidine pathway used by *Pseudomonas*. The intermediate pseudooxynicotine is the direct precursor of a potent tobacco-specific lung carcinogen (6, 9, 10).

In addition, a novel pathway of nicotine degradation in a fungi strain was recently proposed, and it is different from bacterial degradation pathways (Fig. 1*C*) (11). In our previous work, a *nic* gene cluster encoding nicotine oxidoreductase (NicA) and HSP hydroxylase (HspA) from *Pseudomonas putida* S16 was cloned and expressed in *Escherichia coli* (6, 12). HspA (312 amino acids) was interesting because it had low amino acid identity to any proteins of known function (12, 13). The enzyme HspA activity was relatively low (0.75 μM min^{-1} DHP production mg^{-1} protein) (12, 13). It made us search for another, more active HSP hydroxylase.

* This work was supported in part by Chinese National Natural Science Foundation Grants 30900042 and 30821005 and from Ministry of Science and Technology of China National Basic Research Program Grant 2009CB118906. This work was also supported by Key Basic Research Program of Shanghai Grant 09JC1407700 and Grant 10CG10 from the Chen Guang Project from the Shanghai Municipal Education Commission and the Shanghai Education Development Foundation.
[S] The on-line version of this article (available at http://www.jbc.org) contains supplemental text, Tables S1 and S2, and Figs. S1 and S2.
[1] These authors contributed equally to this work.
[2] To whom correspondence should be addressed: School of Life Sciences and Biotechnology, Shanghai Jiao Tong University, Shanghai 200240, China. Tel.: 86-21-34206723; Fax: 86-21-34206723; E-mail: pingxu@sjtu.edu.cn

[3] The abbreviations used are: HSP, 6-hydroxy-3-succinoylpyridine; DHP, 2,5-dihydroxy-pyridine.

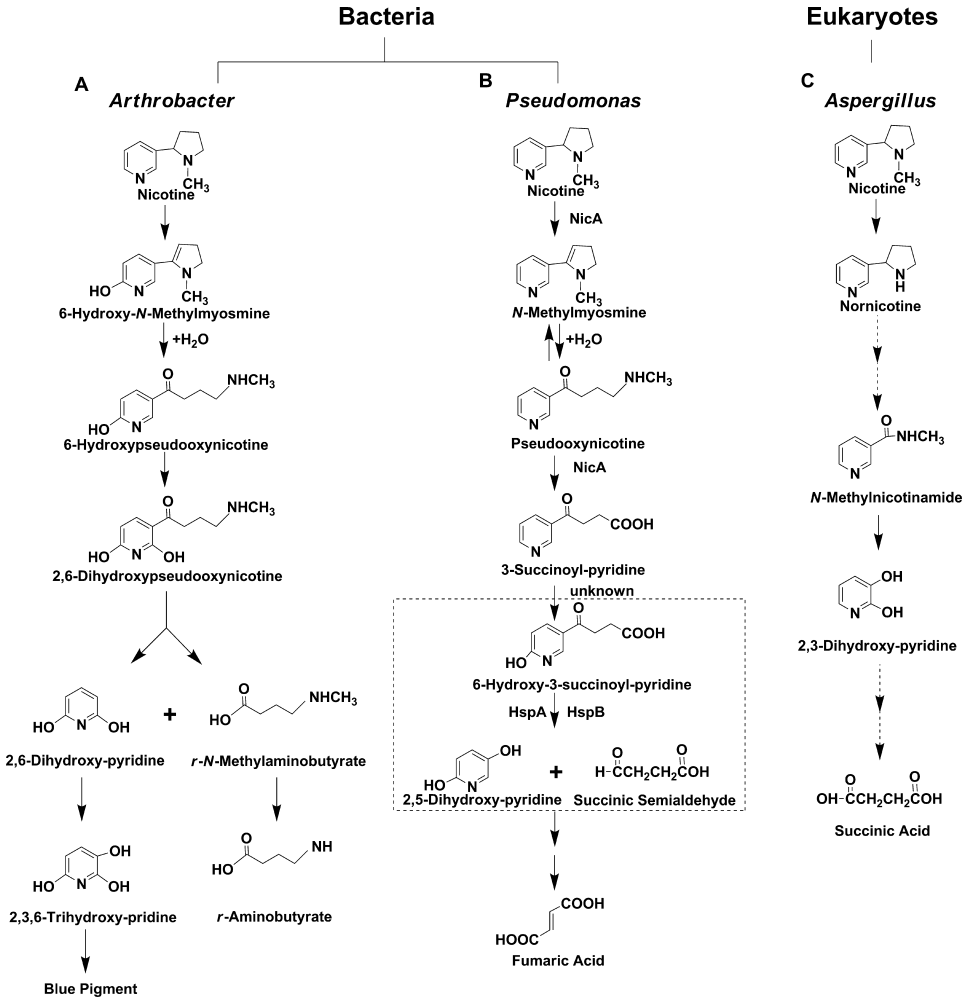

FIGURE 1. **Proposed pathways for nicotine degradation in *Pseudomonas*, *Arthrobacter*, and eukaryotes.** *A*, in *Arthrobacter nicotinovorans*. *B*, in *Pseudomonas*. The reaction in the *dashed frame* is catalyzed by the HSP hydroxylases, HspA and HspB. *C*, in *Aspergillus oryzae*.

In this study, we describe another HSP hydroxylase (HspB) that has low amino acid identity (10.9%) to HspA. The catalytic efficiency of HspB is higher than that of HspA (12). $^{18}O_2$ labeling experiments gave direct evidence for the incorporation of oxygen from O_2 into the DHP produced. The enzyme HspB contains FAD as a prosthetic group, depends on reduced NADH as coenzyme, acts on HSP, and consumes 1 mol of O_2/mol of NADH. Deleting *hspB* but not *hspA* prevented nicotine catabolism by *P. putida* S16, demonstrating the importance of the newly discovered HspB. The work described here provides a sound basis for future studies aimed at a better understanding of the molecular principles of nicotine degradation.

EXPERIMENTAL PROCEDURES

Materials

L-(−)-Nicotine (99% purity) was obtained from Fluka Chemie GmbH. FAD and NADH were obtained from Sigma-Aldrich. $^{18}O_2$ was from Shanghai Research Institute of Chemical Industry. DHP was from SynChem OHG. HSP was isolated and purified from the culture broth of strain S16 (8). Source 30Q, Source 15ISO, and Sephadex G-25, Mono Q 5/50 GL, and Sephacryl S-200 HR columns were from GE Healthcare.

Bacterial Strains and Culture Conditions

P. putida S16 was isolated and cultured at 30 °C in lysogenic broth (LB) medium containing 1 g liter^{-1} nicotine as described previously (14). *E. coli* cells were grown at 37 °C in LB medium, and kanamycin was used for selection at appropriate concentrations.

DNA Manipulation and Gene Isolation

DNA manipulation and transformation were performed according to standard procedures (15). Individual genes were isolated by PCR using template DNA from the corresponding microorganism. The primers are listed in Table 1.

Draft Genome Sequence of P. putida S16

Genomic DNA was sequenced using the Solexa GA platform located at the Helmholtz Center for Infection Research in Germany. The short reads were assembled using Velvet (16) and Edena (17) algorithms. Putative protein-coding regions were predicted by Glimmer 3.01 (18).

HspB Purification

HspB activity was determined at 25 °C by measuring NADH oxidation in a quartz cuvette at 340 nm (NADH, ϵ_{340} = 6220

TABLE 1
Primers

Primer	Sequence (5′-3′)	Recombinant plasmid
hspB	5′-caaccatggcaatgagcatgaaacagcgcgtaat-3′ 5′-cctgcgctcgagacagaaaggtttccatagtctctg-3′	pET28a-*hspB*
hspB mutation	1: 5′- atgagcatgaaacagcgcgtaattatcg-3′ 2: 5′-tctcgacgcacgaagctattgattaaccaatccccttcgacaat-3′ 3: 5′-attgtcgaaggggattggttaatcaatagcttcgtgcgtcgaga-3′ 4: 5′-cagaaaggtttccatagtctctggaa-3′	*hspB* mutant
hspB deletion	5′-gcaggaattcgtctgttcgggtagttcttgg-3′ 5′-gatagtcgacgtaacgcgctggtgcattc-3′	S16-*hspB* deletion
hspA deletion	5′-cagtgaattctcgaccctgaaaatccggac-3′ 5′-gatagtcgacatggttggtttcctccctg-3′	S16-*hspA* deletion

TABLE 2
HspB purification from *P. putida* S16

Step	Total volume	Total protein	Total activity	Specific activity	Yield	Purification factor
	ml	*mg*	*nkat*	*nkat mg^{-1}*	*%*	*Fold*
Crude extract	190	2,380	2063	0.833	100	1
Ammonium sulfate treatment	32.5	485	1511	3.17	73.3	4
Anion exchange I (Source 30Q)	46.3	62.4	1400	22.5	67.9	27
Hydrophobic interaction (Source 15ISO)	8.7	10.2	1258	123	61.0	148
Anion exchange II (Mono Q)	1.2	5.6	1100	197	53.3	236
Gel filtration (Sephacryl S-200 HR)	2.6	3.0	635	212	30.8	254

M^{-1} cm^{-1}) using a UV-visible 2550 spectrophotometer (Shimadzu, Kyoto, Japan). The assay mixture was composed of 1.0 mM HSP, 0.25 mM NADH, and 10 μM FAD in 50 mM Tris-HCl buffer, pH 8.0. The Tris-HCl buffer was made at 25 °C. The reaction was initiated by the addition of enzyme. One katal of enzyme activity represents the oxidation of 1 mol of NADH/second. All manipulations of purification of wild-type HspB were performed at 4 °C, and all chromatography steps were carried out using an ÄKTA purifier chromatography system (GE Healthcare). All buffers contained 1 mM DTT, 1 mM EDTA, and 10 μM FAD. The cells were resuspended in 50 mM Tris-HCl buffer, pH 8.0 (50 g of cell paste in 200 ml of buffer), and lysed by sonication (175 W, 20 min). The purification steps were as follows.

Ammonium Sulfate Precipitation—After centrifugation (12,000 × *g*, 30 min), the supernatant was partially precipitated by slowly adding saturated ammonium sulfate solution to a final concentration of 40% saturation at 4 °C. The precipitate was removed by centrifugation, and more saturated ammonium sulfate was added to 50% saturation. Precipitated proteins were collected, dissolved in Tris-HCl buffer (50 mM, pH 8.0), and dialyzed overnight in the same buffer at 4 °C for further purification.

First Anion Exchange Chromatography—After dialysis, the protein solution was applied to a 1.6 × 10-cm Source 30Q anion exchange column pre-equilibrated with Tris-HCl buffer (50 mM, pH 8.0), and eluted with a linear gradient of 0 to 1.0 M NaCl in the same buffer. HspB was eluted at a NaCl concentration of 0.2 M.

Hydrophobic Interaction Chromatography—Active fractions from the previous step were pooled and supplemented with ammonium sulfate to a final concentration of 30% saturation. The supernatant was loaded onto a Source 15ISO column (0.5 × 11 cm) pre-equilibrated with 30% ammonium sulfate solution in 50 mM Tris-HCl buffer, pH 8.0. HspB was eluted using a reverse linear ammonium sulfate gradient from 30 to 0%. Active fractions were obtained from 27 to 25% saturation, pooled, and desalted on a Sephadex G-25 column (1.6 × 2.5 cm) in 50 mM Tris-HCl buffer, pH 8.0. We note that a substantial loss of activity occurred when FAD was omitted from the buffers.

Second Anion Exchange Chromatography—The desalted enzyme solution was applied to a Mono Q column (0.5 × 5 cm), using the same equilibration and elution conditions as the first anion exchange chromatography step. Activity was detected in fractions containing 0.35 M NaCl, and the solution was concentrated by ultrafiltration. The 10-kDa ultrafiltration tube was purchased from Millipore (Millipore Corporation, Billerica, MA).

Gel Filtration—Finally, the concentrated solution was loaded onto a Sephacryl S-200 HR column (1.6 × 60 cm) pre-equilibrated with Tris-HCl buffer (50 mM, pH 8.0) containing 150 mM NaCl. HspB was eluted using the same buffer at 0.45 column volume. Purified enzyme fractions were stored at −20 °C until further use.

Electrophoresis and Cross-linking

SDS-PAGE was performed using a 12.5% gel in a MiniProtean III electrophoresis cell (Bio-Rad) (19). Native PAGE was performed using gradient gels with a polyacrylamide range from 5 to 12.5% to determine the composition of the enzyme solution. Cross-linking of enzyme subunits was carried out by adding glutaraldehyde to the enzyme solution (20). Glutaraldehyde (1.5 μl, 1%, w/v) was added to 60 μl of enzyme solution (4 g liter^{-1}) and incubated for 12 h at room temperature.

NH_2-terminal Amino Acid Sequence of HspB

The NH_2-terminal amino acid sequence of the enzyme was determined using automated Edman degradation (Shanghai Ji Kang Corp., Shanghai, China).

HspB Cofactor Determination

The flavin cofactor of HspB was identified and quantitatively analyzed by HPLC (Agilent 1200 series; Hewlett-Packard Corp., Santa Clara, CA) as described previously (21). The protein-containing solution (1.4 g liter^{-1}) was boiled for 3 min to

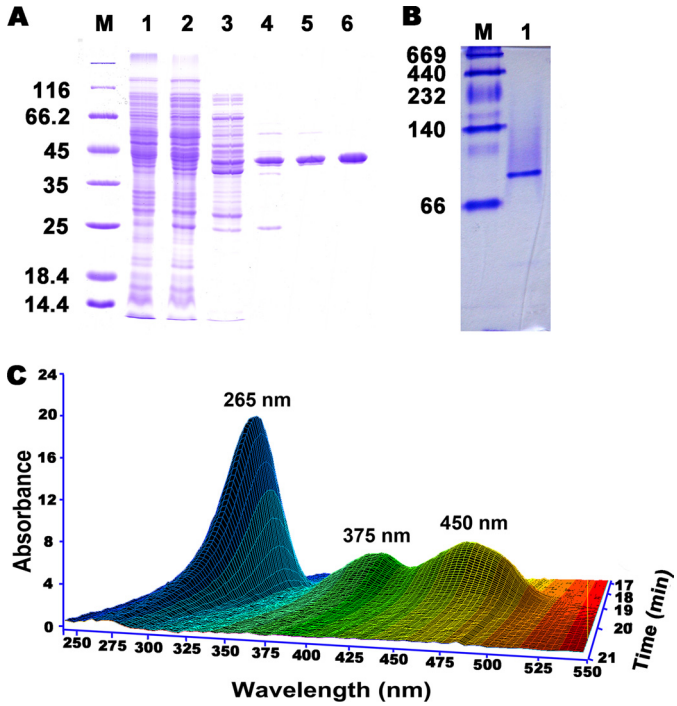

FIGURE 2. **Purification of HspB.** *A*, SDS-PAGE. *Lane M*, marker proteins; *lane 1*, *P. putida* S16 cell extract; *lane 2*, supernatant from $(NH_4)_2SO_4$ precipitation; *lane 3*, source 30Q pool; *lane 4*, source 15ISO pool; *lane 5*, Mono Q fraction; *lane* 6, Sephacryl S-200 HR fraction. *B*, native PAGE of purified HspB. *Lane M*, native protein marker; *lane 1*, purified HspB. *C*, three-dimensional plot of HPLC analysis for FAD from the boiled HspB solution.

isolate the cofactor, which was detected by HPLC equipped with an Eclipse XDB-C18 column (4.6 × 150 mm; particle size, 5 μm) and diode array detection. The eluent was 100 mM ammonium bicarbonate, 18% methanol. A solution of the same composition, excluding HSP hydroxylase, was also measured as a control because extra FAD was used during the entire purification procedure. Standard FAD solutions of 0.1, 0.2, 0.4, 0.6, and 1.0 mM were used for quantitative analysis and detected at 265 nm.

$^{18}O_2$ Incorporation

To confirm enzymatic decarboxylation and monooxygenation of HSP, $^{18}O_2$ was incorporated into DHP, which was the reaction product. The reaction was performed in a flask sealed by a plug with two rubber tubes for gas flow. Tris-HCl buffer (50 mM, pH 8.0) containing 1.0 mM HSP, 0.25 mM NADH, and 10 μM FAD was injected into the flask. The air in the flask was replaced by a flow of continuous nitrogen gas. Next, $^{18}O_2$ was injected, and enzyme solution was added to the buffer to initiate the reaction, which was then stopped by heating. As a control, another flask containing $^{16}O_2$ from air was used. After precipitate removal by centrifugation (12,000 × *g*, 30 min), the supernatants were analyzed by direct insertion mass spectra recorded on an API 4000 LC-MS system (Applied Biosystems, Foster City, CA).

Oxygen Consumption

HspB oxygen consumption was measured polarographically using a Chlorolab 2 system (Hansatech Instruments, Norfolk,

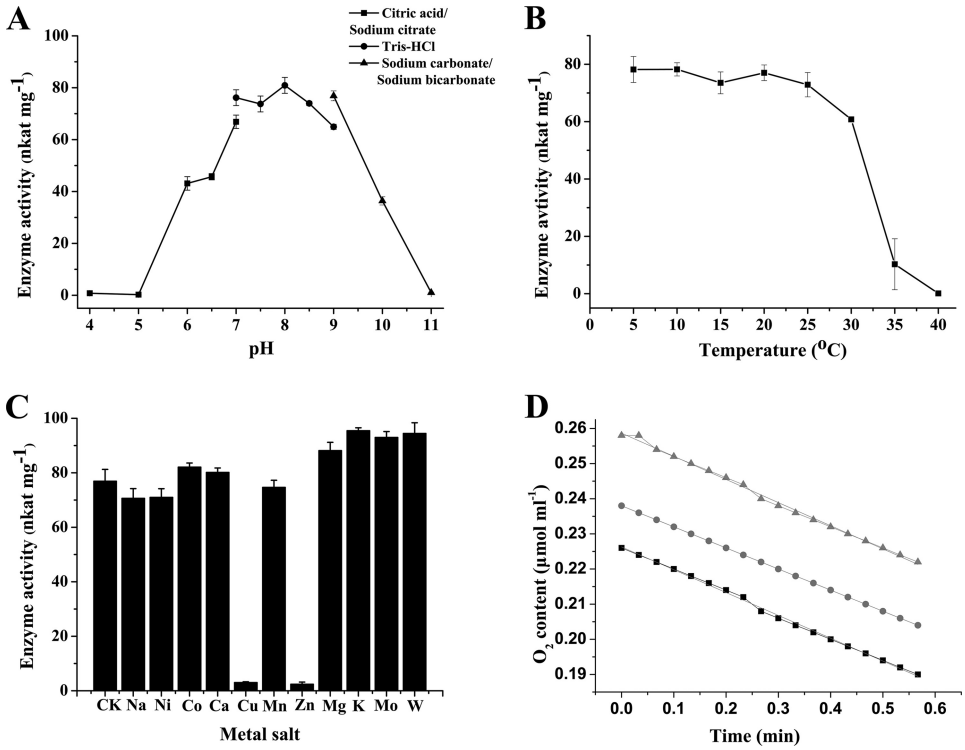

FIGURE 3. **Characterization of HspB.** *A*, pH dependence of HspB stability. The enzyme was incubated overnight in buffers of various pH at 25 °C. *B*, thermostability of HspB. The enzyme was incubated in Tris-HCl buffer (50 mM, pH 8.0) at varying temperatures for 30 min. *C*, effects of metal salts on HspB stability. *CK*, without metal salt; *Na*, Na^+; *Ni*, Ni^{2+}; *Co*, Co^{2+}; *Ca*, Ca^{2+}; *Cu*, Cu^{2+}; *Mn*, Mn^{2+}; *Zn*, Zn^{2+}; *Mg*, Mg^{2+}; *K*, K^+; *Mo*, MoO_4^{2-}; *W*, WO_4^{2-}. *D*, oxygen consumption of the HspB reaction. ▲, ●, and ■ indicate the oxygen declines from different initial concentrations. For the above four experiments, enzyme activity was determined according to the standard assay at 25 °C and pH 8.0.

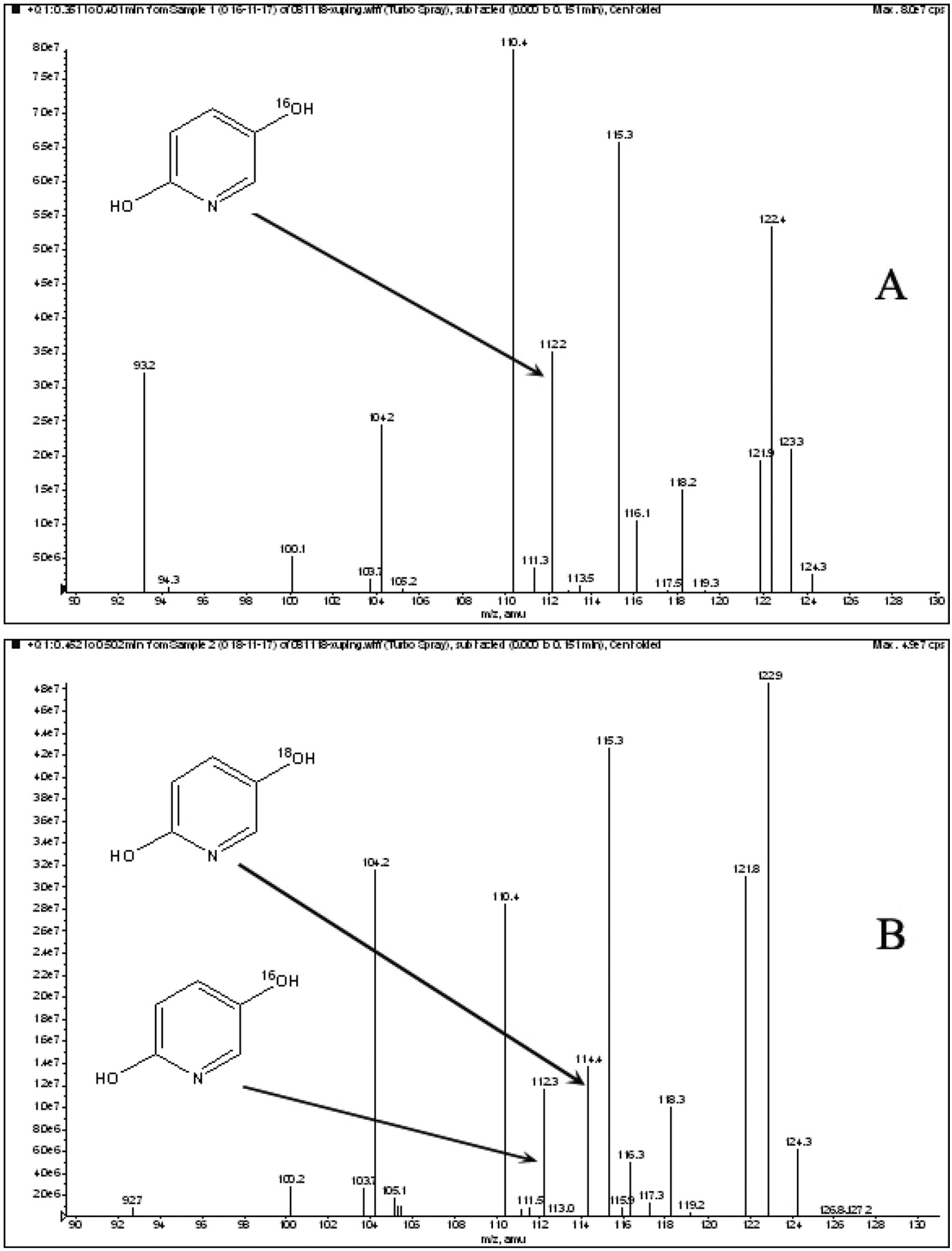

FIGURE 4. **Mass spectra of DHP as determined by LC-MS analysis.** The mass spectra of derived DHP are obtained from reactions without $^{18}O_2$ (*A*) and with $^{18}O_2$ (*B*). The positions of the peaks for [^{18}O] DHP are indicated by *arrows*.

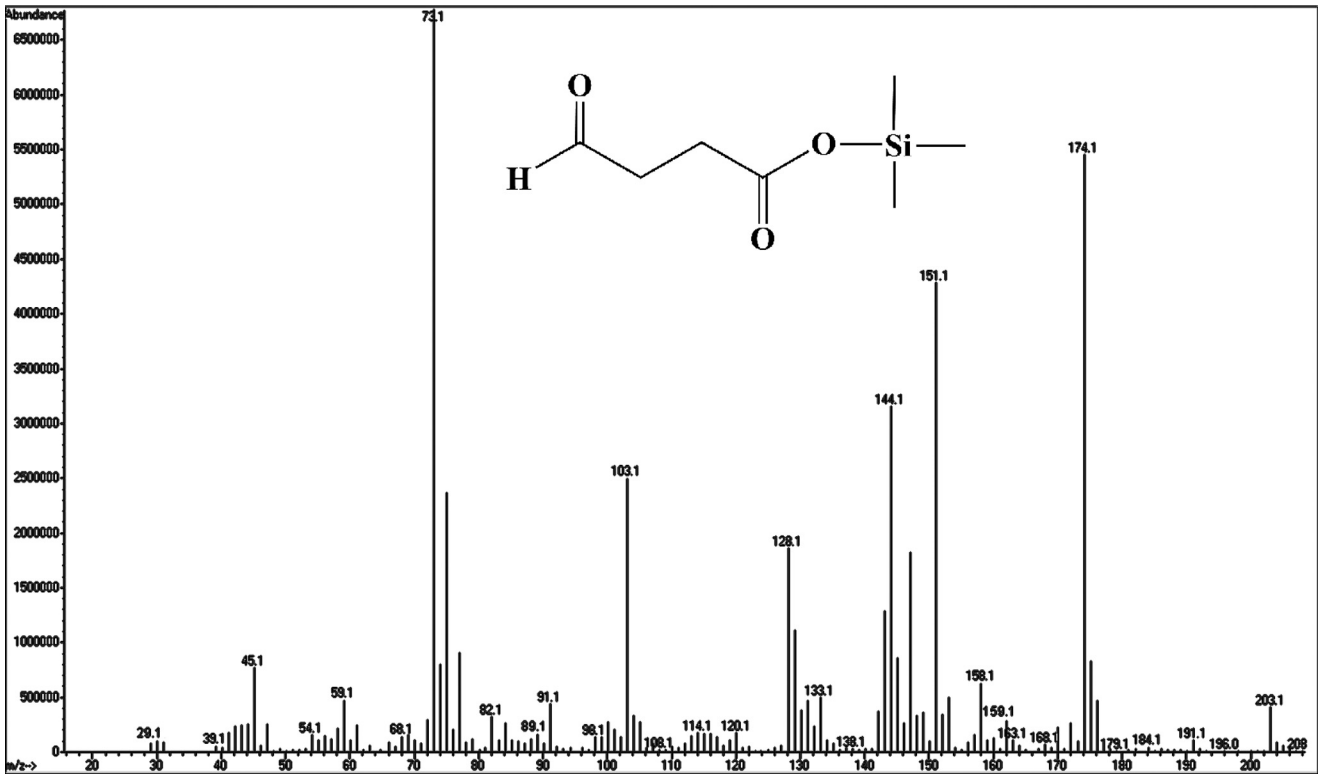

FIGURE 5. **Mass spectrum of succinic semialdehyde as determined by GC-MS analysis.** The GC-MS determination with derivatization of silanization by special peak is as follows. A molecular ion peak is seen at *m/z* 174, and its fragments are at *m/z* 29 ($[CHO]^+$), 45 ($[COOH]^+$), 89 ($[Si(CH_3)_3O]^+$), and 73 ($[(CH_2)_2COOH]^+$).

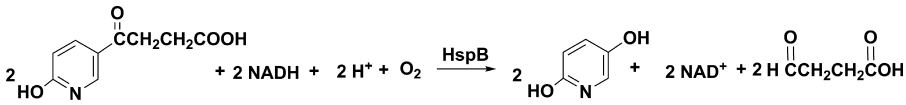

FIGURE 6. **HSP degradation catalyzed by HspB.**

UK). The reaction mixture contained 1.0 mM HSP, 0.25 mM NADH, 10 μM FAD, 50 mM Tris-HCl buffer (pH 8.0) and an appropriate concentration of enzyme HspB. The reaction was completed after 1 min, and HSP consumption was measured by HPLC.

P. putida S16 Mutant (hspA and hspB) Gene Deletion

To delete the *hspA* and *hspB* genes in strain S16 by single homologous recombination, internal fragments were amplified by PCR and cloned into the polylinker region of pK18mob (Table 1). To transfer the pK18mob into strain S16, triparental filter mating was performed as described previously using *E. coli* DH5α as the donor strain, *E. coli* HB101 (pRK2013) as the helper strain, and strain S16 as the recipient strain (22). *P. putida* S16 exconjugants harboring disrupted genes were isolated on M9 minimal medium plates containing citrate and kanamycin after incubation at 30 °C for 12 h. All of the mutant strains were analyzed by PCR to confirm target gene disruption.

HspB Site-directed Mutagenesis

The GADGA motif was deleted using the recombinant PCR method; the primers are listed in Table 1. Wild-type and mutant *hspB* genes were subcloned separately between the NcoI-XhoI sites of the pET28a expression vector. The crude cell enzymatic activity was detected as described above.

Analytical Techniques

HSP and DHP were detected by HPLC and confirmed by direct-insertion mass spectra recorded on the API 4000 LC-MS system. HPLC analysis was performed with a mobile phase of the mixture of methanol and 1 mM acetic acid (25:75, v/v) at a flow rate of 0.5 ml min^{-1}. MS analysis was performed in both negative and positive ion turbo ion spray ionization mode.

Succinic semialdehyde was detected by GC-MS (GCD 1800C; Hewlett Packard, Folsom, CA) equipped with a 50 m J&W DB-5MS column, operated at 140 °C. The injection port and detector were set at 260 and 280 °C, respectively. After the HspB enzyme reaction, the reaction mixture (1 ml) was evaporated to dryness at 50 °C under reduced pressure and dissolved in 200 μl of acetonitrile. The acetonitrile solution was transferred to a vial and dried under a stream of nitrogen. The residue was silylated by the addition of 200 μl of bis(trimethylsilyl)-trifluoroacetamide (Sigma-Aldrich) at 80 °C for 4 h. After drying under a stream of nitrogen, the sample was redissolved in acetonitrile. Samples were analyzed by GC-MS.

Nucleotide Sequence Accession Number

The nucleotide sequence reported in the present study has been deposited in GenBank™ under accession number GQ857548.

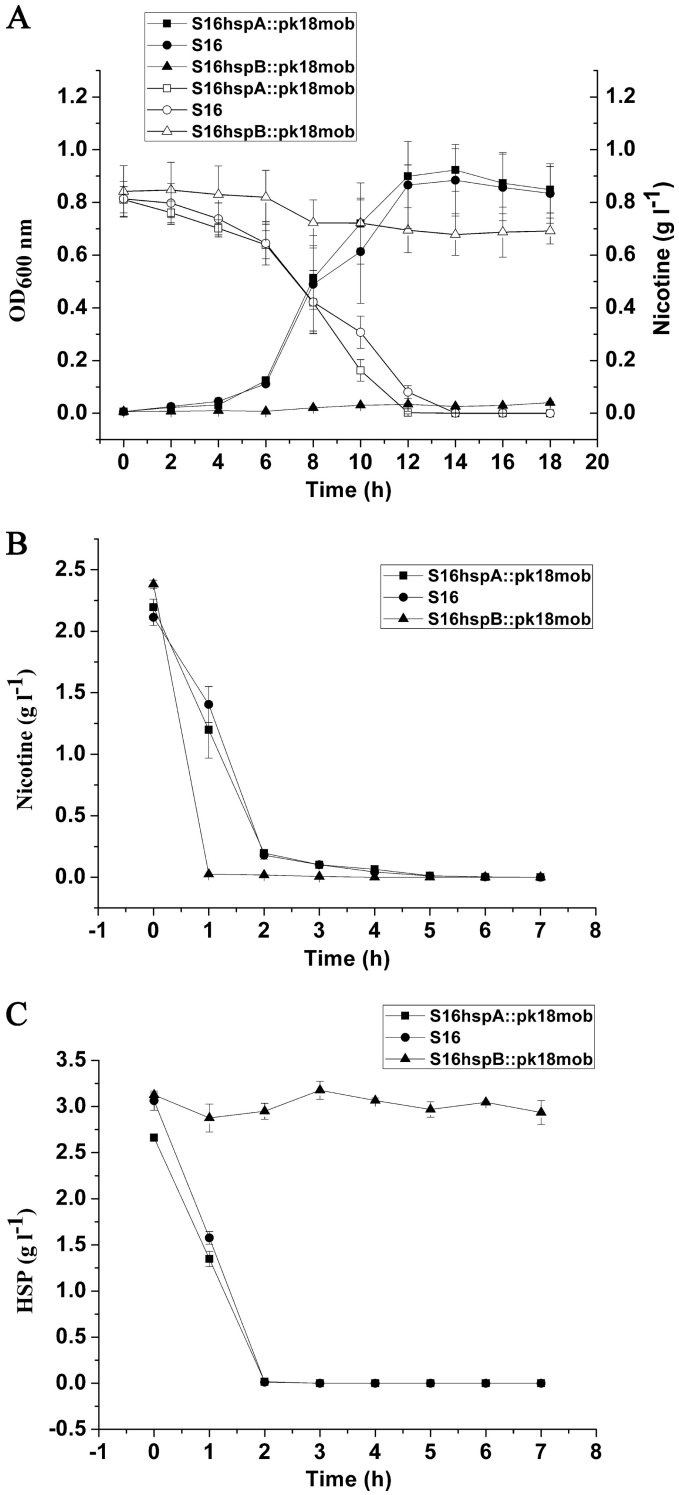

FIGURE 7. **Cell growth and resting cell reactions of strain S16 and the gene deletion mutants.** *A*, utilization of nicotine for growth by S16 *hspA*::pk18mob (deletion of *hspA*), S16 (as control), and S16 *hspB*::pk18mob (deletion of *hspB*). ■, cell growth of S16 *hspA*::pk18mob (deletion of *hspA*); ●, cell growth of S16 as control; ▲, cell growth of S16 *hspB*::pk18mob (deletion of *hspB*); □, nicotine concentration in the medium for S16 *hspA*::pk18mob growth; ○, nicotine concentration in the medium for S16 growth as control; △, nicotine concentration in the medium for S16 *hspB*::pk18mob growth. *B*, resting cell reactions of S16 *hspA*::pk18mob (deletion of *hspA*), S16 (as control), and S16 *hspB*::pk18mob (deletion of *hspB*) in nicotine degradation. ■, nicotine concentration in the medium for S16 *hspA*::pk18mob degradation; ●, nicotine concentration in the medium for S16 degradation as control; ▲, nicotine concentration in the medium for S16 *hspB*::pk18mob degradation. *C*, resting cell reactions of S16 *hspA*::pk18mob (deletion of *hspA*), S16 (as control), and S16 *hspB*::pk18mob (deletion of *hspB*) in HSP degradation. ■, HSP concentration in the medium for S16 *hspA*::pk18mob degradation; ●, HSP concentration in the medium for S16 degradation as control; ▲, HSP concentration in the medium for S16 *hspB*::pk18mob degradation. The values are the means of three replicates, and the *error bars* indicate the standard deviations.

RESULTS AND DISCUSSION

Analysis of genes and biochemical characterization of nicotine catabolism enzymes forms a basis for rationally improving *Pseudomonas* strains employed in nicotine waste disposal (13, 23). The characterization of genes and gene products in nicotine degradation by *Pseudomonas* will lead to a full understanding of this catabolic activity. The previously studied HSP hydroxylase (HspA) had a relatively low specific activity, which made us search for another, more active HSP hydroxylase (12).

HspB Purification and hspB Identification

The HSP hydroxylase was assayed by measuring NADH oxidation. HspB was purified ~250-fold in five steps with an overall yield of 30%, using conventional column chromatography (Table 2). HspB had a molecular mass of ~40 kDa on SDS-PAGE (Fig. 2*A*) and 80 kDa when determined by native Sephacryl S-200 HR column chromatography or by native PAGE of the purified enzyme (Fig. 2*B*). SDS-PAGE of the enzyme solution treated with glutaraldehyde produced a strong band at 40 kDa and a weaker band at 80 kDa, indicating partial cross-linking (supplemental Fig. S1). These data suggest that HspB is a dimer.

The NH_2-terminal amino acid sequence of purified HspB was SMKQRVIIVG. The *hspB* gene sequence was identified by mining of the *P. putida* S16 draft sequence and comparing it with the NH_2-terminal sequence of HspB. The newly discovered *hspB* gene is separated by more than 30 kb of DNA away from the *nic* gene cluster, which contains *nicA* and *hspA* (6, 12). The HspB gene product displays 10.9% amino acid identity with HspA (12). NCBI BLASTP analysis revealed the identity of HspB to *p*-nitrophenol monooxygenase from *Pseudomonas* sp. NyZ402 (41% amino acid identity) (24).

Prosthetic Group Identification

HspB is predicted to contain an FAD-binding domain (Pfam01494, amino acids 30–336) according to NCBI Blast. The HspB sequence was submitted to the mGenThreader server for fold assignment, and the protein structures with significant hits were chosen as templates for further modeling (Table S1). Five models were generated, and the one with the lowest discrete optimized protein energy score was chosen for visualization (Table S2). The three-dimensional structure is the NCBI-curated FAD domain in pfam01494 (supplemental Fig. S2, *A* and *B*). Further experimental evidences supported the involvement of FAD in the function of HspB. First, HspB UV-visible maximum absorbance at 382 and 452 nm with a minimum at 410 nm is characteristic of a flavoprotein (data not shown). Second, the three-dimensional plot of diode array detection data shows that the supernatant of the boiled enzyme solution exhibited absorption maxima at 265, 375, and 450 nm, identical to FAD (Fig. 2*C*). Third, the FAD concentration in

purified HspB (33 μM) was 36 μM (calculated from the 265-nm peak), suggesting that each HspB subunit contains one FAD as a prosthetic group. Besides, the addition of FMN did not affect enzyme activity (data not shown). Based on further sequence analysis, we found a GADGA motif (amino acids 162–166) in the FAD-binding domain (supplemental Fig. S2*C*). The mutant *hspB* without the GADGA motif was inserted into pET28a and expressed in *E. coli* BL21(DE3). The transformant pET28a-*hspB* served as a positive control. No HspB activity of the transformant containing mutant *hspB* was detected in both cell free extract and resting cells. This result indicates the importance of the GADGA motif in the FAD-binding domain.

Characterization of HspB Reaction Conditions

Effect of pH on HspB stability—HspB activity was measured after overnight incubation at 25 °C in buffers with identical ionic strength (50 mM) at different pH. Citric acid-sodium citrate, Tris-HCl, and sodium carbonate-sodium bicarbonate buffers were used for incubation at pH 4.0–7.0, 7.0–9.0, and 9.0–11.0, respectively. The enzyme displayed maximal stability in Tris-HCl buffer (pH 8.0) (Fig. 3*A*). At pH below 7.0 or above 9.0, there was substantial loss of activity. Phosphate buffer (pH 6.0–8.0), which was used initially, clearly inhibited enzyme activity (not shown).

Effect of Temperature on HspB Stability—To assess temperature stability, HspB was incubated in Tris-HCl buffer (50 mM, pH 8.0) for 30 min at temperatures ranging from 5 to 40 °C. The enzyme activity measured at 5 °C was maintained up to ~25 °C but was lost quickly at higher temperatures (Fig. 3*B*). The enzyme was stable for at least 1 week at 4 °C in Tris-HCl buffer and for several months frozen in the same buffer at −20 °C (not shown). Optimal pH and temperature for enzyme catalysis were pH 8 and 25 °C, respectively. The specific activity of the purified enzyme under optimal conditions was ~4.8 μmol of NADH oxidized min^{-1} mg^{-1}.

Effects of Metal Salts on HspB Activity—The effect of 11 metal salts at 2 mM (Na^+, Ni^{2+}, Co^{2+}, Ca^{2+}, Cu^{2+}, Mn^{2+}, Zn^{2+}, Mg^{2+}, K^+, MoO_4^{2-}, and WO_4^{2-}) on HspB activity was examined. Cu^{2+} and Zn^{2+} completely abolished enzyme activity, but the other ions had minimal inhibitory effects (Fig. 3*C*), suggesting that HspB did not require a metal cofactor.

Characterization of HspB Reaction Mechanism

$^{18}O_2$ Labeling—The HspB reaction was performed in the presence of $^{18}O_2$ to confirm the predicted incorporation of a single oxygen atom into DHP. The reaction products were analyzed by LC-MS. The fragmentation pattern was consistent with the incorporation of one ^{18}O into DHP at position 5 (Fig. 4).

HspB Reaction Product "Succinic Semialdehyde" Detection—After derivatization by silanization, the product of the HspB reaction was analyzed by GC-MS. The molecular ion peak is at *m*/*z* 174, and featured fragments are at *m*/*z* 29 ($[CHO]^+$), 45 ($[COOH]^+$), 89 ($[Si(CH_3)_3O]^+$), and 73 ($[(CH_2)_2COOH]^+$) (Fig. 5).

Reaction Kinetics of HspB—HSP concentration was 0.2 mM when we measured the K_m for NADH. The concentration for NADH was 0.25 mM when we measured the K_m for HSP. Kinetic constants for the enzyme showed apparent K_m = 0.175 mM, k_{cat} = 2.0 s^{-1} for HSP in the presence of NADH, and no detectable activity in the presence of NADPH. HSP acts as an initial effector and strongly stimulates NADH oxidation by HspB (apparent K_m = 0.104 mM).

HSP Oxidation Stoichiometry—The reaction stoichiometry of HSP oxidation by HspB was calculated from NADH consumption, oxygen consumption (Fig. 3*D*), and HSP degradation. The ratio of oxygen (0.64 μmol) consumption and NADH (1.3 μmol) oxidation was 1:2. HSP degradation was measured by HPLC, and ~0.89 μmol of HSP was consumed for each 0.74 μmol of NADH oxidized. Therefore, the ratio of NADH used for HSP oxidation was ~1:1 (Fig. 6).

Deletion of hspA and hspB Genes

The *hspA* and *hspB* genes were deleted separately, and the related cell growth and resting cell reactions were all performed. The *hspA* gene deletion mutant could grow well in nicotine medium as the same as wild-type strain S16, whereas the *hspB* gene deletion mutant could not grow in nicotine medium (Fig. 7*A*). Cells of *hspA* and *hspB* gene deletion mutants were harvested in the mid-growth phase by centrifugation at 6,000 × *g* for 10 min at 4 °C, washed three times with 0.02 M sodium phosphate buffer (pH 7), and suspended in the same buffer at 5 of $A_{600\ nm}$ (called resting cells). Resting cells of *hspA* and *hspB* gene deletion mutants could both transform nicotine (Fig. 7*B*) to HSP. In addition, resting cells of *hspB* gene deletion mutant could not degrade HSP, different from *hspA* gene deletion mutant and strain S16 (Fig. 7*C*). The above facts indicate that HspB is crucial for HSP transformation and nicotine degradation by the strain. Isoenzymes present in bacteria are thought to be involved in substrate distribution as well as reducing equivalents among different intracellular compartments (25). Additionally, the *hspA* and *hspB* genes are located in different gene clusters. We propose that these two enzymes may be isoenzymes coexisting in the same cell. The HspB enzymatic mechanism might be similar to the oxidative decarboxylation reaction of 6-hydroxynicotinate catalyzed by 6-hydroxynicotinate 3-monooxygenase, depending on O_2, NADH, and FAD, except that HspB cannot degrade 6-hydroxynicotinate (26).

In summary, a novel hydroxylase was purified and mechanistically characterized, and the gene encoding the enzyme was identified. This study demonstrates the importance of the discovered enzyme that is crucial for nicotine degradation by the *Pseudomonas* strain.

Acknowledgments—We thank Dr. Tobias Kieser (John Innes Centre, Norwich, UK) and two anonymous reviewers for very helpful comments on the manuscript. We also acknowledge Dr. Helmut Bloecker for draft genome sequencing at the Helmholtz Center for Infection Research (Braunschweig, Germany).

REFERENCES

1. Novotny, T. E., and Zhao, F. (1999) *Tob. Control* **8,** 75–80
2. Díaz, E., Ferrández, A., Prieto, M. A., and García, J. L. (2001) *Microbiol. Mol. Biol. Rev.* **65,** 523–569
3. Díaz, E. (2004) *Int. Microbiol.* **7,** 173–180

4. Brandsch, R. (2006) *Appl. Microbiol. Biotechnol.* **69,** 493–498
5. Eberhardt, H. (1995) *Beitr. Tabakforsch. Int.* **16,** 119–129
6. Tang, H., Wang, L., Meng, X., Ma, L., Wang, S., He, X., Wu, G., and Xu, P. (2009) *Appl. Environ. Microbiol.* **75,** 772–778
7. Wang, S. N., Liu, Z., Tang, H. Z., Meng, J., and Xu, P. (2007) *Microbiol. SGM* **153,** 1556–1565
8. Wang, S. N., Xu, P., Tang, H. Z., Meng, J., Liu, X. L., and Qing, C. (2005) *Environ. Sci. Technol.* **39,** 6877–6880
9. Hecht, S. S., Hochalter, J. B., Villalta, P. W., and Murphy, S. E. (2000) *Proc. Natl. Acad. Sci. U.S.A.* **97,** 12493–12497
10. Hukkanen, J., Jacob, P., 3rd, and Benowitz, N. L. (2005) *Pharmacol. Rev.* **57,** 79–115
11. Meng, X. J., Lu, L. L., Gu, G. F. and Xiao, M. (2010) *Res. Microbiol.* **161,** 626–633
12. Tang, H., Wang, S., Ma, L., Meng, X., Deng, Z., Zhang, D., Ma, C., and Xu, P. (2008) *Appl. Environ. Microbiol.* **74,** 1567–1574
13. Li, H., Li, X., Duan, Y., Zhang, K. Q., and Yang, J. (2010) *Appl. Microbiol. Biotechnol.* **86,** 11–17
14. Wang, S. N., Xu, P., Tang, H. Z., Meng, J., Liu, X. L., Huang, J., Chen, H., Du, Y., and Blankespoor, H. D. (2004) *Biotechnol. Lett.* **26,** 1493–1496
15. Sambrook, J., and Russell, D. W. (2001) Molecular Cloning: A Laboratory Manual, 3rd Ed., Cold Spring Harbor Laboratory, Cold Spring Harbor, NY
16. Zerbino, D. R., and Birney, E. (2008) *Genome Res.* **18,** 821–829
17. Hernandez, D., François, P., Farinelli, L., Osterås, M., and Schrenzel, J. (2008) *Genome Res.* **18,** 802–809
18. Delcher, A. L., Harmon, D., Kasif, S., White, O., and Salzberg, S. L. (1999) *Nucleic Acids Res.* **27,** 4636–4641
19. Laemmli, U. K. (1970) *Nature* **227,** 680–685
20. Griffith, I. P. (1972) *Biochem. J.* **126,** 553–560
21. Eppink, M. H., Boeren, S. A., Vervoort, J., and van Berkel, W. J. (1997) *J. Bacteriol.* **179,** 6680–6687
22. Tao, F., Yu, B., Xu, P., and Ma, C. Q. (2006) *Appl. Environ. Microbiol.* **72,** 4604–4609
23. Civilini, M., Domenis, C., Sebastianutto, N., and Bertoldi, M. (1997) *Waste Manag. Res.* **15,** 349–358
24. Wei, Q., Liu, H., Zhang, J. J., Wang, S. H., Xiao, Y., and Zhou, N.Y. (2010) *Biodegradation* **21,** 575–584
25. Hunter, G. R., Hellman, U., Cazzulo, J. J., and Nowicki, C. (2000) *Mol. Biochem. Parasitol.* **105,** 203–214
26. Nakano, H., Wieser, M., Hurh, B., Kawai, T., Yoshida, T., Yamane, T., and Nagasawa, T. (1999) *Eur. J. Biochem.* **260,** 120–126